BIOCHEMISTRY
including biophysical chemistry & molecular biology
Article

*Biochemistry* **2009,** *48,* 10457–10466 10457
DOI: 10.1021/bi901052c

# Temperature Dependence of the Reduction of $P_{700}^+$ by Tightly Bound Plastocyanin in Vivo†

Stefano Santabarbara,*,‡,§,∥ Kevin E. Redding,‡ and Fabrice Rappaport§

‡*Department of Chemistry and Biochemistry, Arizona State University, 1711 South Rural Road, Tempe, Arizona 85287, and* §*Institut de Biologie Physico-Chimique, UMR7141 CNRS-Universite Paris 6, 13 Rue Pierre et Marie Curie, 75005 Paris, France.* ∥*Present address: Department of Physics, University of Strathclyde, John Anderson Building, 107 Rottenrow East, Glasgow G4 0NG, Scotland, United Kingdom.*

*Received June 22, 2009; Revised Manuscript Received September 23, 2009*

ABSTRACT: The kinetics of reduction of $P_{700}^+$, the stably oxidized electron donor of Photosystem I, by plastocyanin (PC) has been investigated by pump−probe optical spectroscopy in living cells of the green alga *Chlamydomonas reinhardtii*, between 277 and 318 K. The reduction of $P_{700}^+$ in vivo is described by two kinetic components with lifetimes of $6 \pm 0.5$ and $56 \pm 1$ $\mu$s at room temperature. The rapid reduction phase, which is attributed to reduction of $P_{700}^+$ by prebound PC, is thermally activated with an apparent activation barrier of 105−115 meV. The analysis of the in vivo reaction is consistent with (i) reduced PC and PS I forming a relatively tight binary complex that does not undergo kinetically limiting conformational reconfiguration and (ii) the activation barrier being determined principally by enthalpic contributions to the free energy change. Under the approximation that entropic contributions to the free energy change associated with this electron transfer reaction are negligible, a lower boundary value of the reorganization energy is estimated to be 0.54−0.63 eV, which is on the lower range of the distribution for intraprotein electron transfer reactions. This low activation barrier is discussed in terms of the optimization of primary donor reduction.

Electron transfer (ET)[1] reactions are of fundamental importance in bioenergetics. In biological systems, ET involves the movement of an electron from donor to acceptor molecules which are bound to proteins in a relatively rigid structure, so that the cofactors are often separated by distances which exceed the molecular radii. Hence, the diffusion of the electron acceptor and donor molecules, as well as the direct overlap of the molecular orbitals of the electron transfer partners, is hindered. Therefore, for the reaction to take place, the electrons need to tunnel through a potential energy barrier (reviewed in refs (*1*−*3*)). The oxidation and reduction of diffusible electron carriers can also proceed through the tunneling processes (reviewed in refs (*1*−*5*)), even though it involves the movement of electrons between different cofactor−protein complexes.

The simpler description of the rate of electron tunneling, in the nonadiabatic limit, is given by the modification of the semiclassical formulation, introduced by Marcus (*6*), which includes the quantum-mechanical coupling with solvent phonons (*7*−*9*):

$$k_{et} = \frac{2\pi |V_{AD}|^2}{\hbar\sqrt{2\pi}\vartheta(T)} e^{-(\Delta G^\circ + \lambda_t)^2/(2\vartheta^2(T))} \quad (1)$$

where $V_{AD}$ is the electronic coupling matrix element between the electron donor (D) and the electron acceptor (A) molecule, $\lambda_t$ is the (total) reorganization energy, and $\vartheta$(T) is the width of the Gaussian curve describing the Franck−Condon factors.

The ET rate would show an extremely weak temperature dependence when $\Delta G^\circ = -\lambda$. Still, $k_{et}$ may depend on $T$, because of the $\vartheta$(T) term which in its most simple formulation is described by

$$\vartheta^2(T) = \hbar\bar{\omega}\lambda_t \coth \frac{\hbar\bar{\omega}}{2k_b T} \quad (2)$$

where $k_b$ is the Boltzmann constant, $\bar{\omega}$ is the mean phonon mode expressed in angular frequency units, and $T$ is the absolute temperature. When $k_bT$ is larger than $\hbar\bar{\omega}$, $\vartheta^2$(T) tends to $2\lambda_t k_b T$. As a result, eq 1 becomes equivalent to the classical derivation of Marcus (*6*):

$$k_{et} = \frac{2\pi |V_{AD}|^2}{\hbar\sqrt{4\pi\lambda_t k_b T}} e^{-(\Delta G^\circ + \lambda_t)^2/(4\lambda_t k_b T)} \quad (3)$$

However, when $\hbar\bar{\omega} \gg k_bT$ (i.e., tunneling is coupled to high-frequency phonon modes), $\vartheta^2$(T) tends to a constant value ($\hbar\bar{\omega}\lambda_t$), so that the ET rate becomes effectively temperature-independent (*1*, *2*, *7*). More accurate expressions, which consider full quantum-mechanical coupling with one (*9*) or more frequency modes (*1*, *2*, *5*), as well as specific tunneling pathways within the inhomogeneous protein medium (e.g., refs *10* and *11*), have also been discussed.

Even though the rate of ET depends, in principle, on a limited number of parameters, accurate determination of the electronic coupling factor ($V_{AD}$) and total reorganization energy ($\lambda_t$) has

†This study was funded in part by a grant (DE-FG02-08ER15989) from the Department of Energy and a CAREER award (MCB-0854851) from the National Science Foundation to K.E.R.

*To whom correspondence should be addressed. E-mail: stefano.santabarbara@strath.ac.uk. Telephone: 0141 552 3074. Fax: 0141 552 2891.

[1]Abbreviations: cyt, cytochrome; ET, electron transfer; PS I, Photosystem I; $PhQ_A$ and $PhQ_B$, phylloquinones A and B, respectively; $F_X$, $F_A$, and $F_B$, iron−sulfur clusters X, A, and B, respectively; $P_{700}^+$, Photosystem I primary donor (cation); $PC^{II}$, oxidized plastocyanin; $PC^I$, reduced plastocyanin; RC, reaction center; $\lambda_t$, (total) reorganization energy; $k_{et}$, electron transfer rate.


Published on Web 09/24/2009

often proved to be difficult, yet to a first approximation, the value of $|V_{AD}|^2$ depends exponentially on the distance between the acceptor and donor molecules (*3*, *5*, *12*), scaled by a factor known as the tunneling barrier. Moreover, for systems in which the spatial arrangement of cofactors and the intervening medium is known with sufficient resolution, computational approaches based on ab initio quantum-chemical and molecular dynamics calculations (reviewed in refs *14* and *15*) can also be employed.

Information relating to other parameters determining the Franck−Condon factors (i.e., the reorganization energy and the mean phonon mode coupled to electron donor and acceptor) can be, in principle, retrieved from the analysis of the temperature dependence of the ET reaction, particularly when the free energy change can be assessed from independent investigation. A survey of intraprotein ET reactions involving redox-active centers of numerous enzymes, including photosynthetic complexes, has led to average values of $\lambda_t$ in the range of 0.6−0.7 eV (*3*, *5*, *14*, *15*). Nevertheless, considerably lower values (∼0.2 eV) were determined for ultrafast photochemical charge separation reactions, particularly in the reaction centers of purple bacteria (see ref *16* and references cited therein). Values of $\lambda_t$ lower than 200 meV were also reported for the reduction of the cyt $a_3$−$Cu_B$ binuclear center in cytochrome *c* oxidase (*17*). On the other hand, the reorganization energy appears to increase for interprotein ET, which typically occurs on the microsecond time scale, with average values close to 1 eV (*3*−*5*). A complication associated with the analysis of interprotein ET reactions is that they often display polyphasic kinetics, reflecting diffusion-limited complex formation and heterogeneity of prebound acceptor−donor complexes (reviewed, e.g., in refs (*18*−*20*)). Still, the rates of the more rapid interprotein ET reactions taking place from preformed complexes have often been successfully described by tunneling theory (e.g., refs (*1*−*5*) and *21*). This observation suggests that, within the time of the ET reaction, the binary donor−acceptor complex is stable enough for the Franck−Condon approximation employed in the derivation of the theoretical formulation to hold true. When this is the case, interprotein ET reactions can be treated analogously to intraprotein ET, for which the geometrical arrangement of the cofactor is defined by their binding to the protein matrix.

Probably the most extensively investigated interprotein ET reactions in photosynthetic systems are the donation of an electron from cytochrome $c_2$ (cyt $c_2$) to the primary donor of the purple bacterial reaction center (reviewed in ref *23*) and the reduction of ferredoxin (reviewed in ref *24*) by the acceptor side of Photosystem I (PS I). The reduction of the PS I primary donor $P_{700}^+$ by the diffusible carrier plastocyanin (PC) (reviewed in refs (*18*−*20*)) and cyt $c_6$ (*19*, *20*) has also been extensively investigated in vitro. However, studies performed in vivo are far less abundant and have, in certain cases, produced results contradictory to investigations in purified systems (*25*, *26*). Crystallographic structures of supercomplexes composed of PS I and its acceptor ferredoxin (*27*) and that of cyt $c_2$ and the reaction center (RC) of *Rhodobacter sphaeroides* (*28*, *29*) have been reported, supporting the formation of a tight binary complex. However, at present, the crystallization of a binary complex between PC and PS I has been unsuccessful.

The lower boundary value of the reorganization energy associated with the reduction of $P_{700}^+$ by reduced plastocyanin ($PC^I$) was estimated to be 545 meV, based on the effect of site-directed mutants with altered $P_{700}$ redox potential in whole cells of *Chlamydomonas reinhardtii* (*30*). Even considering the relatively small range of $\Delta G°$ values (−77 to −217 meV) explored in the study of Ramesh and co-workers (*30*), the lower bound value of $\lambda_t$ appears to fall on the low edge of the spread reported for interprotein ET and is particularly low, considering that the reaction involves ET between different proteins, and that the redox-active center of PC is a Cu atom. Similar lower boundary values of $\lambda_t \cong 500$ meV were reported for another intercomplex reaction, the reduction of the oxidized primary donor in the RC of *R. sphaeroides* ($P_{870}^+$) by cyt $c_2$, analyzing the effect of altering the driving force of the reaction (*31*). However, a successive investigation that took into account the temperature dependence of the ET rates measured in the same mutants, where $\Delta G°$ was varied between −65 and −420 meV, yielded a larger $\lambda_t$ value of $\cong$920 ± 110 meV (*21*). This latter value close to ∼1 eV is consistent with the temperature dependence of the $P_{870}^+$ reduction previously measured in *R. sphaeroides* wild-type reaction centers (*32*).

We have reinvestigated in whole cells of *C. reinhardtii* the temperature dependence of $P_{700}^+$ reduction by prebound $PC^I$. We estimate the activation enthalpy of the reaction ($\Delta H^‡$ = 100−110 meV). Making the assumptions that (i) the high-temperature limit is an adequate description of the ET rate for the conditions employed in this study and (ii) the entropic contribution to the free energy difference is negligible, so that $\Delta H^‡ \approx \Delta G^‡$, we estimate the lower bounds for the total reorganization energy to be 525−620 meV. The relatively small value of $\lambda_t$ leads to an acceleration of $P_{700}^+$ reduction by 2 orders of magnitudes compared to what it would be if the average value for interprotein electron transfer (∼1 eV) held true.

## EXPERIMENTAL PROCEDURES

The *C. reinhardtii* strain containing the *FuD7* (*psbA*Δ) mutation in the *P71* low-antenna background, which accumulates wild-type levels of PS I and cyt $b_6f$, was used in these experiments. Cells were grown heterotrophically in TAP medium, which contains acetate as a carbon source. They were harvested by centrifugation at 1500*g* for 5 min and immediately resuspended to a concentration equivalent to 1.5 OD units at 678 nm (the peak in the $Q_y$ absorption band of chlorophyll *a*) in 50 mM Hepes-NaOH (pH 8) buffer containing Ficoll (20%, w/v) to prevent sedimentation of the cells during the measurements. The uncoupler FCCP was added at a final concentration of 10 $\mu$M to collapse the transmembrane ionic gradients. The temperature of the samples was controlled with a circulating water bath. The sample was left to incubate for 15 min once the temperature was reached before the kinetics were recorded.

*Time-Resolved Difference Absorption Spectroscopy*. The kinetics of electron transfer in whole cells of *C. reinhardtii* were recorded using a pump−probe spectrometer, which has been previously described in detail (*34*). In brief, the excitation pulse is provided by a Nd:YAG pumped dye (LDS 698) laser. The excitation wavelength was set to 700 nm and the intensity regulated by a neutral metal grid so as to excite approximately 70% of the complexes during the ∼6 ns actinic pulse. The kinetics were probed at discrete wavelengths, using the output of an OPO (Panther, Continuum) pumped by a frequency-tripled Nd:YAG laser (Surelite I, Continuum). The temporal resolution of the instrument is better than 7 ns, without deconvolution of the actinic pulse profile.

*Analysis of ET Kinetics at Room Temperature*. The kinetics (monitored every 5 nm in the 350−540 nm range) at 298 K were globally fitted by a sum of exponentials:

$$\Delta A(t,\lambda) = \sum_{i=1}^{n} a_i(\lambda) e^{-tk_i} + b(\lambda) \quad (4)$$

where $a_i(\lambda)$ is the amplitude (at wavelength $\lambda$) of the decay-associated spectrum (DAS) with (apparent) rate constant $k_i$ and $b(\lambda)$ is the amplitude (at wavelength $\lambda$) of the DAS of the nondecaying component. All DAS are reported in Figure S1 of the Supporting Information.

*Analysis of the Temperature Dependence of ET Kinetics*. (*i*) *Global Analysis*. At each temperature investigated, in the 277−318 K interval, the kinetics recorded at 430, 445, 460, and 480 nm were fitted simultaneously (globally) by a fit function of the form of eq 4, but which explicitly describes the temperature dependence: $\Delta A(t,\lambda,T) = \sum_{i=1}^{n} a_i(\lambda,T) e^{-tk_i(T)} + b(\lambda,T)$. In this type of analysis, the rate constants $k_i(T)$ are only global fit parameters (i.e., they assume the same value for each wavelength investigated, at a given temperature), while the amplitudes of the DAS are unconstrained. The thermodynamic parameters associated with the temperature dependence of the reaction were extracted by the Arrhenius plot of $\ln[k_i(T)]$ as a function of $T^{-1}$. (The Arrhenius relation is often expressed as $k_i(T) = k_{max} e^{-E_a/k_b T}$ where $E_a$ is the activation barrier and $k_{max}$ is the maximal rate constant. It is easily shown that, in this form, $E_a \approx \Delta H^{\ddagger}$, the activation free enthalpy difference, rather than $E_a \approx \Delta G^{\ddagger}$, the activation free energy difference, and that the pre-exponential term is $k_{max} = k_{max}^{eff} e^{\Delta S^{\ddagger}}/k_b$.

(*ii*) *Global-Target Analysis*. In the global-target analysis, which is analogous to the case of global analysis, the data are fitted to the function $\Delta A(t,\lambda,T) = \sum_{i=1}^{n} a_i(\lambda,T) e^{-tk_i(T)} + b(\lambda,T)$ However, while in the global analysis no particular assumption is made about the temperature dependence of the rate constants, in global-target analysis, a theory-based assumption is introduced: $k_i(T)$, which is described by eq 1, in the high-temperature approximation ($k_b T > \hbar\bar{\omega}$), reduces to

$$k_i(T) = CT^{-1/2} e^{-\Delta H^{\ddagger}/k_b T} \quad (5)$$

where $C$ is a temperature-independent constant, equivalent to $C = C' e^{\Delta S^{\ddagger}}/k_b$, where $C' = \pi^{1/2}|V_{AD}|^2/[\hbar(k_b\lambda_t)]$ and $\Delta S^{\ddagger}$ is the activation entropy difference. Equation 5 is equivalent to eq 1 (in the high-temperature limit) but does not require any assumption about the specific value of $\lambda_t$, which is implicitly contained in the terms $C'$ and $\Delta G^{\ddagger} = \Delta H^{\ddagger} - T\Delta S^{\ddagger}$. With this definition of $k_i(T)$, all kinetic data sets, monitored between 430 and 480 nm, and in the 277−318 K temperature range, are fitted simultaneously. Thus, the rate constant $k_i(T)$ is not a fit parameter in the global-target analysis; it is described by the values of $C$ and $\Delta H^{\ddagger}$, which are common to all data sets. The amplitudes $a_i(\lambda,T)$ and $b(\lambda,T)$ are, as for the non-model-based global analysis, unconstrained. The principal advantage of the global-target analysis is that, as all data are fitted simultaneously, the number of possible numerical solutions, and hence the errors in the parameter estimates, are largely reduced (*35*). Second, the activation enthalpy ($\Delta H^{\ddagger}$) is extracted directly from the fitting rather than from subsequent analysis, which also increases the precision of the estimation.

The data were fitted by laboratory-written software operating in MatLab, which minimizes the reduced sum of the squared residuals, using a combination of the Simplex (initial search) and Levenberg−Marquardt (refine minimization) algorithms. Errors are estimated by the Covariance matrix, and the stability of the solution was tested by an iterative search as described by Beechem (*35*) and Venturoli et al. (*21*).

## RESULTS

The temperature dependence of the light-induced ET kinetics in the PS I reaction center was investigated in living cells of *C. reinhardtii* by pump−probe transient optical spectroscopy. The kinetics were monitored at four discrete wavelengths in the 430−480 nm range and from 5 ns to 20 $\mu$s after the pump flash, after incubation of the cells at a set temperature. These wavelengths were selected as they allowed preferential monitoring of the kinetics of either $P_{700}^{+}$ reduction (430 and 445 nm) or the electro-chromic band shift (ECS, 460 and 480 nm) associated with vectorial electron transfer in the PS I RC (e.g., ref *36*). The latter process (ECS) dominates the kinetics at wavelengths longer than 460 nm, and although it does not directly monitor $PhQ^{-}$ oxidation, it has been shown to relax with exactly the same kinetic lifetimes as the actual ET reaction, as expected from its electrochromic origin (see DAS in Figure S1 of the Supporting Information as well as refs (*36*−*39*)). Furthermore, it has been shown that, in vitro, the activation barriers of the $PhQ^{-}$ oxidation reaction estimated from the temperature dependence of the kinetics recorded at 480 nm (ECS) and 390 nm ($PhQ^{-}$) are virtually indistinguishable (*40*).

Figure 1 shows the transient flash-induced absorption changes as well as the global-target fits at selected temperatures. A satisfactory description of the experimental data at all wavelengths requires at least three exponential decay components, which are characterized by lifetimes of 20 ± 1 ns, 228 ± 6 ns, and 6.3 ± 0.2 $\mu$s at 298 K, in agreement with previous investigations of the same organism at room temperature (Figure S1 of the Supporting Information and refs *35* and *36*). On the basis of the differential absorption in the near UV, the 20 and 228 ns components have been assigned to the oxidation of phyllosemiquinone ($PhQ^{-}$) molecules bound by the PsaB and PsaA subunits, respectively (*36*−*39*), and the 6.3 $\mu$s phase has been assigned to the reduction of $P_{700}^{+}$ by prebound $PC^{I}$ on the basis of the bleaching at 432 nm (e.g., refs *36* and *37*).

Figure 2A also shows the Arrhenius plot of the rate derived from the global-target fitting of the experimental results as a function of temperature. The temperature dependence of the amplitudes associated with each of the kinetics components at the four wavelengths investigated is reported in Figure S2 of the Supporting Information. As the data are subjected to a model-based analysis (see Experimental Procedures for further details), the activation enthalpies ($\Delta H^{\ddagger}$) are extracted directly from the fitting of the kinetics acquired at different set temperatures, and they are determined to be 47.1 ± 0.5, 107 ± 2, and 104.5 ± 0.1 meV for the 20 ns, 228 ns, and 6.3 $\mu$s components, respectively.

Also shown in Figure 2A (△) is the Arrhenius plot of the 6.3 $\mu$s phase for an unconstrained three-exponential fit, which shows that even dropping the assumption of particular temperature dependencies of the rate constants does not much influence the result of the fits. The value of $\Delta H^{\ddagger}$ is 106.2 ± 0.8 meV in this case. However, the value of the lifetimes of the fast (~20 ns) and slow (~230 ns) phases of $PhQ^{-}$ reoxidation retrieved from the free-running, three-exponential fit displayed a significant statistical

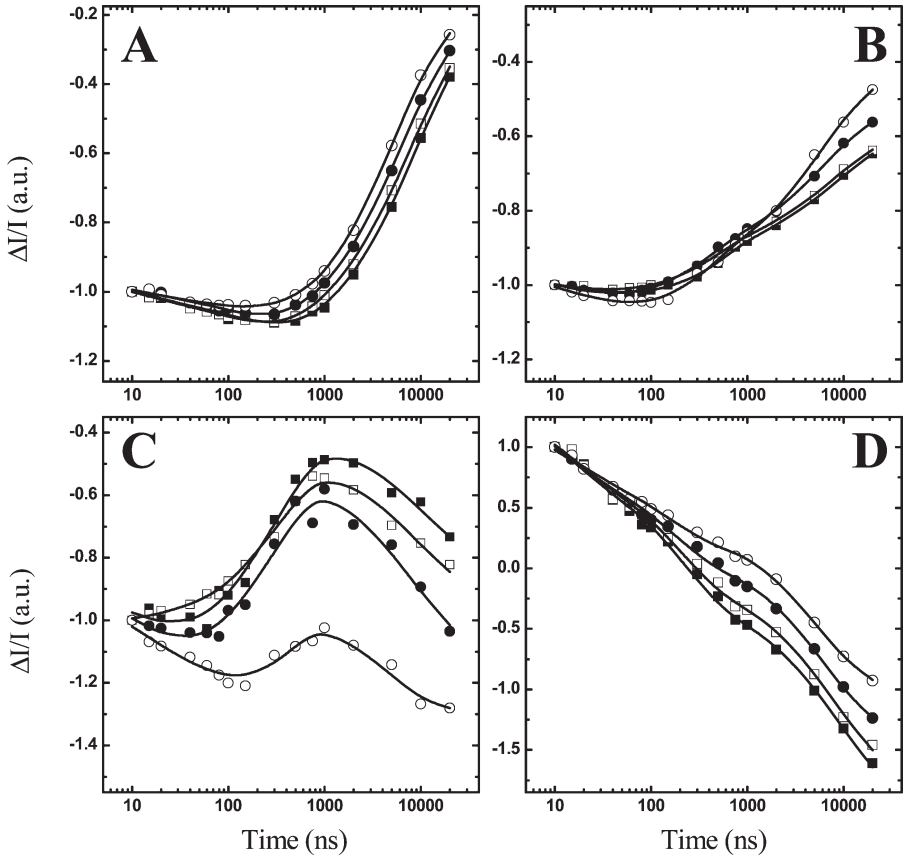


FIGURE 1: Temperature dependence of the kinetics of light-induced ET in PS I monitored at 430 (A), 445 (B), 460 (C), and 480 nm (D), in living *C. reinhardtii* cells maintained at 277 (■), 288 (□), 298 (●), or 305 K (○). Solid lines are the global fit to the experimental results considering a four-exponential decay model.

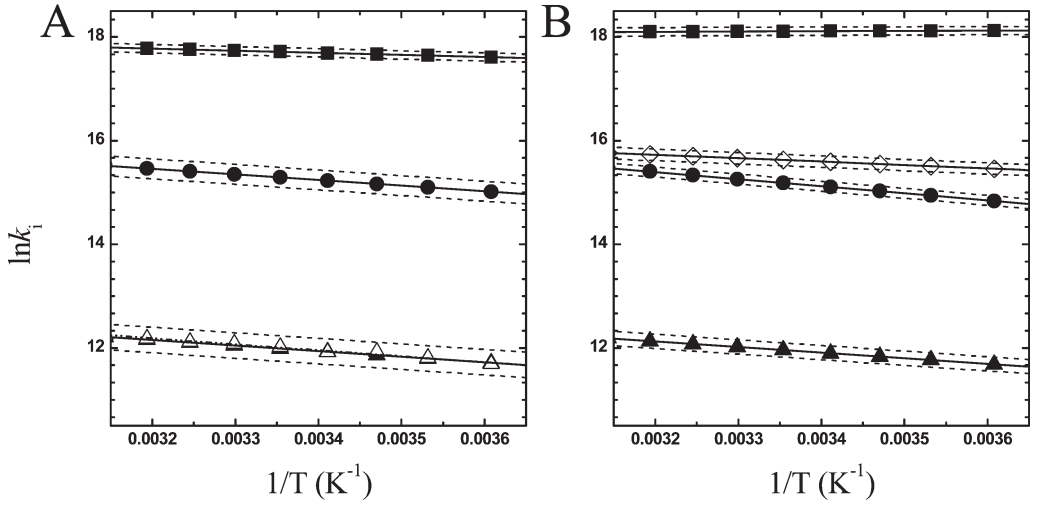


FIGURE 2: Dependence of the apparent rate constants upon temperature, shown as conventional Arrhenius plots. (A) Rate constants obtained from a three-exponential global-target fit: (■) $\tau_{1,298K}$ = 20.3 ns ($C = 5.32 \times 10^9$ s$^{-1}$ K$^{1/2}$), (●) $\tau_{2,298K}$ = 228 ns ($C = 4.61 \times 10^9$ s$^{-1}$ K$^{1/2}$), and (▲) $\tau_{3,298K}$ = 6.2 $\mu$s ($C = 1.67 \times 10^8$ s$^{-1}$ K$^{1/2}$). Empty triangles represent an unconstrained global fit ($\tau_{3,298K}$ = 6.3 $\mu$s). (B) Rate constants obtained from a four-exponential global-target fit: (■) $\tau_{1,298K}$ = 13.6 ns ($C = 1.79 \times 10^9$ s$^{-1}$ K$^{1/2}$), (●) $\tau_{2,298K}$ = 255 ns ($C = 1.56 \times 10^9$ s$^{-1}$ K$^{1/2}$), (◇) $\tau_{3,298K}$ = 164 ns ($C = 1.08 \times 10^{10}$ s$^{-1}$ K$^{1/2}$), and (▲) $\tau_{4,298K}$ = 6.4 $\mu$s ($C = 1.68 \times 10^8$ s$^{-1}$ K$^{1/2}$). For both panels, the solid lines are extrapolations from the fitting parameters for the temperature dependence of the rates while the dashed lines mark the confidence interval (within 2$\sigma$). For the unconstrained analysis of the ~6 $\mu$s component shown in panel A, the dashed−dotted line is the linear regression through the data points, the slope of which ($E_a k_b^{-1}$) is obtained from the derivation of ln $K_{et}$, which is $E_a = \Delta H^{\ddagger} - k_b T/2$.

scatter, albeit distributed around the same average value obtained from the model-based fitting approach (Figure S3 of the Supporting Information).

Figure 2B shows the Arrhenius plot obtained from fitting the experimental data with a four-exponential function (the amplitudes are shown in Figure S2). An additional decay component was considered, based on prior results from the investigation of both the temperature dependence of $PhQ^-$ oxidation in purified cyanobacterial PS I (*40*) and the effects of $PhQ_A$ site mutations in living *C. reinhardtii* cells (*38*, *39*), which revealed the presence of an intermediate component with a $\tau$ of ≈170−180 ns. At 298 K, the best fit to the kinetics is obtained with lifetimes of 13.7 ± 0.4 ns,

164 ± 6 ns, 255 ± 3 ns, and 6.4 ± 0.2 μs. The activation enthalpies for these four kinetic components are then 8.0 ± 0.5, 69 ± 1, 129.8 ± 0.6, and 105.9 ± 0.3 meV, respectively. After taking into account the contribution of this additional component decaying on the nanosecond time scale, we determined a higher rate for the fast component of $PhQ^-$ oxidation, which is associated with a lower activation barrier, while the slow component is shifted to a slightly slower rate with a larger activation barrier. However, it is important to note that the kinetics of $P_{700}^+$ reduction, and the associated $\Delta H^‡$ value, are, substantially, independent of the specific kinetic model adopted to fit the transient optical data.

## DISCUSSION

*Temperature Dependence of $PhQ^-$ Oxidation*. Investigation of the temperature dependence of the ET reactions occurring in vivo in the nanosecond-to-microsecond time range in the PS I reaction center allows the determination of the activation enthalpy difference ($\Delta H^‡$) associated with the oxidation of $PhQ^-$ by $F_X$ and with the reduction of $P_{700}^+$ by $PC^I$ prebound to the RC. The values of $\Delta H^‡$ associated with the fast phase of $PhQ^-$ oxidation (8−47 meV), which is attributed to oxidation of $PhQ_B^-$, are in agreement with the conclusions (7−15 meV) drawn from a previous study of PS I RCs isolated from *Synechocystis* sp. PCC 6803 (*40*). A relatively good agreement is also obtained for the slow phase of $PhQ^-$ oxidation, which is attributed to the oxidation of $PhQ_A^-$ (*36*−*41*) and was estimated to be 65−110 meV in isolated particles (*40*). It is noteworthy that the values of $\Delta H^‡$ are relatively insensitive to the specific kinetic model used to describe the experimental data, as shown from the relatively narrow spread of values (107−130 meV) obtained from the analysis using either a three- or four-exponential decay (Figure 2). When the kinetics are fitted with a sum of four exponential functions, larger values of $\Delta H^‡$ (130 meV) for the oxidation of $PhQ_A^-$ are obtained compared to the value extracted from the three-component fitting (106 meV). A comparable difference is observed for the fast phase (20 ns) attributed to oxidation of $PhQ_B^-$. Thus, after taking into account the intermediate component (∼160 ns), we found the apparent activation of the fast (∼20 ns) and slow (∼200 ns) components, attributed to $PhQ_A^-$ and $PhQ_B^-$, respectively, is in very close agreement with the estimates obtained in cyanobacterial PS I RCs (*40*).

The additional kinetic phase is characterized by a lifetime of ∼164 ns at 298 K, in agreement with the previous investigation of mutations of the $PhQ_A$ binding site in *C. reinhardtii* (*38*, *39*) and the investigation of the temperature dependence of $PhQ^-$ oxidation in isolated cyanobacterial PS I (*40*). This kinetic component was tentatively attributed to the oxidation of reduced $F_X$ by the terminal acceptors ($F_A$ and $F_B$ (*38*, *39*)). The presence of two closely spaced lifetime components in the midnanosecond range in the wild-type reaction center has also been predicted by kinetic simulations of the $PhQ^-$ oxidation kinetics, based on electron tunneling theory (*42*). However, in the previous investigation performed in isolated cyanobacterial PS I RCs (*40*), it was not possible to evaluate the activation energy associated with this intermediate component, because of excessive statistical scatter in the fitted lifetimes. From our fitting of the in vivo kinetics in *C. reinhardtii*, we estimate that $\Delta H^‡$ = 69 meV for this component, which is hardly negligible. This also explains the difference in $\Delta H^‡$ calculated for the slow component (∼200 ns) of $PhQ^-$ oxidation using different kinetic models, since the estimated value would tend toward the weighted average of the unresolved lifetimes when the ∼160 ns component is neglected.

To apply electron tunneling theory reliably to experimentally determined activation barriers (and maximal rates), the free energy difference ($\Delta G°$) and the rate constant of the individual reaction should be accurately known. Neither of these two requirements is met in the case of the $PhQ^-$ oxidation reactions (see the reviews in refs (*42*−*44*) for more extensive discussion of this issue), precluding any further application of electron transfer theory to the experimental results at this stage.

*Temperature Dependence of $P_{700}^+$ Reduction by Prebound $PC^I$*. The reduction of $P_{700}^+$ in vivo, which is characterized by a lifetime of ∼6 μs at 298 K, exhibits a clear temperature dependence that is satisfactorily described by an activation enthalpy difference ($\Delta H^‡$) of 105−110 meV (Figure 2). Since the reduction of $P_{700}^+$ requires the formation of a binary complex between PS I and $PC^I$, several factors could lead to a thermally activated reaction. These include the equilibrium of PC binding at the PS I luminal side, possible rearrangements of the complex to a metastable "active" intermediate from which ET takes place, and the dependence of the ET rate upon parameters already discussed for interprotein ET reactions.

Most of the previous investigations of $P_{700}^+$ reduction have been performed in isolated systems. The kinetics in vitro are markedly biphasic, showing components of ∼6−20 and 50−150 μs (*18*−*20*). The rate of the fast phase of $P_{700}^+$ reduction is independent of $PC^I$ concentration, as expected for a monomolecular rate constant, while the rate of the slower component increases with an increase in $PC^I$ concentration, indicating the bimolecular character of this reaction (*18*−*20*). Conflicting conclusions have been reached relating to the rate-limiting step of the $P_{700}^+$ reduction reaction. Sigfridsson and coworkers (*45*−*47*) proposed that rearrangement of the PS I−$PC^I$ binary complex imposes the main kinetic constraint in vitro. Structural microrearrangements would require some flexibility of the PS I−$PC^I$ binary complex conformation, such that the active configuration would represent only one of many possible microconformational states. Hence, this process is expected to be associated with a non-negligible entropic contribution to the Gibbs free energy difference, and potentially heterogeneous kinetics due to distributed lifetimes. Diáz and co-workers (*48*) estimated a large value (∼2 meV $K^{-1}$) for the entropy change associated with the bimolecular reduction of $P_{700}^+$ by either $PC^I$ or cyt $c_6^{II}$ and attributed it to ET rather than the binding process. However, Drepper et al. (*33*) argued against the occurrence of significant structural reconfiguration of bound PC at the PS I docking complex, principally because of the absence of kinetic intermediates associated with the reorganization of the binary complex which, for instance, was observed in the case of $P_{870}^+$ reduction by cyt $c_2$ (e.g., refs *23*, *31*, and *32*). The lifetime of the fast $P_{700}^+$ reduction phase was shown to be virtually independent of $PC^I$ concentration (*33*). Only the amplitude of the fast phase increased as a function of $PC^I$ concentration, as expected if it were determined by the binding equilibrium. These results argue against a significant distribution of substrates, as the number of statistically populated microconformational states should scale with the overall $P_{700}^+$−$PC^I$ binary complex concentration but are consistent with the fast phase representing the reaction within a tight preformed complex, limited by the actual ET rate (*33*).

*Occurrence of Kinetic Intermediates Associated with Reconfiguration of the PS I($P_{700}^+$)−$PC^I$ Complex*. To investigate the presence of the aforementioned intermediate

components of $P_{700}^+$ reduction kinetics, we have analyzed the light-induced absorption changes on an extended time scale (up to 250 $\mu$s) and throughout the near-UV and up to 500 nm in the visible abortion spectrum, at room temperature (298 K). The kinetics on the microsecond time scale are described satisfactorily by a biphasic decay characterized by lifetimes of 6 and ~56 $\mu$s. The optical transients and global fits at a few selected wavelengths are shown in Figure 3A, while the DAS of the 6.4 and 56 $\mu$s components are shown in Figure 3B. (The DAS of the nanosecond components were the same as those obtained in the 5 ns to 20 $\mu$s time interval, and hence, they were omitted from Figure 3B.) It is clear that, apart from a difference in amplitude between the DAS of the ~6.4 and ~56 $\mu$s phases, they have similar spectral profiles and are both dominated by the bleaching due to the $P_{700}^+ - P_{700}$ absorption difference (e.g., refs *36*, *49*, and *50*). On the basis of the amplitude of the DAS, we estimate that the fast phase of $P_{700}^+$ reduction (in preformed PS I−$PC^I$ complexes) occurs in >85% of the PS I RCs (Figure 3B). The remainder display a slower $P_{700}^+$ reduction phase with a lifetime of ~56 $\mu$s at 298 K, which we attribute to the bimolecular reaction. This could be limited by PC diffusion, docking of $PC^I$, and release of $PC^{II}$ at the PS I donor side. Thus, the binary complexes of PS I with $PC^I$ represent the vast majority of PS I RCs in dark-adapted cells of *C. reinhardtii*, in agreement with previous investigations (e.g., refs (*36*−*39*)). While we cannot completely exclude the presence of a potential intermediate phase between the ~6 and ~56 $\mu$s phase, it would have to have a small fractional amplitude (<10%) to escape detection.

*Occurrence of the Lifetime Distribution of $P_{700}^+$ Reduction Kinetics*. Structural heterogeneity in the $P_{700}^+ - PC^I$ binary complex would give rise to a distribution of rate constants and hence observable lifetimes (reviewed in ref *51*). This should lead to a deviation from strictly exponential kinetics, which can be accommodated by stretched exponential functions (*51*, *52*). Moreover, as the heterogeneity of the binary population is expected to depend on the temperature, so too will the lifetime distribution. To explore the presence of lifetime (rate) distributions associated with $P_{700}^+$ reduction, we have globally fitted the kinetics acquired at different temperatures using stretched exponentials. This analysis was restricted to the 5 ns to 20 $\mu$s time window, and stretching of the microsecond component only was considered. In the temperature range investigated, the stretching parameter ranged from 0.88 (277 K) to 0.97 (313 K), which indicates a relatively narrow distribution of rate constants (Figure 3C,D). This result is in agreement with experiments performed in PS I isolated from higher plants (*33*). The value of activation enthalpy $\Delta H^{\ddagger}$ obtained from the Arrhenius plot of the mean value of the rate constant, $\langle k(T) \rangle$, is 103 ± 1 meV, which agrees closely with the estimate obtained from global and global-target fits employing simple exponential functions. Thus, although the apparent lifetime of the fast phase of $P_{700}^+$ reduction might still be determined by the kinetics of binary complex reconfiguration, our data provide little support for this hypothesis.

*Estimation of the Reorganization Energy of $P_{700}^+$ Reduction*. If the rate of the fast phase of $P_{700}^+$ reduction were determined exclusively by the ET process, then the temperature dependence of the reaction should be described consistently by electron transfer theory. In Figures 1 and 2, it is shown that the experimental results can be fitted satisfactorily using a simple model based on this theory. The only assumption, justified by the relatively high temperatures employed in these studies, is that the coupling of the ET process with (protein) phonon modes does not deviate from that of a classical nonquantized oscillator. Then, according to Marcus (*6*), the free energy of activation will be defined by the equation

$$\Delta G^{\ddagger} = \frac{(\lambda_t + \Delta G^{\circ})^2}{4\lambda_t} = \frac{(\lambda_t + \Delta H^{\circ})^2}{4\lambda_t} + \frac{(T\Delta S^{\circ})^2}{4\lambda} - \frac{T(\lambda_t + \Delta H^{\circ})\Delta S^{\circ}}{2\lambda_t} \quad (6)$$

The value of $\Delta H^{\ddagger}$, which is determined experimentally, closely approximates that of $\Delta G^{\ddagger}$, which is required to obtain a lower-boundary estimate of $\lambda_t$, when $|\Delta S^{\circ}| \ll |\Delta H^{\circ}|$. A vanishing value of $\Delta S^{\circ}$ might be seen as the absence, or small contribution, of reconfiguration of the solvent (protein scaffold in this case) outside the inner coordination sphere of the redox cofactors (*3*). It is also worth noting that the derivation of eqs 1−3 assumes that the potential surfaces of the donor−acceptor molecules in their ground and ionic states are harmonic and have the same width (*1*−*3*). As explicitly discussed by Hopfield (*8*), this is equivalent to the absence of large entropic (i.e., $\Delta S^{\ddagger} \cong 0$) contributions to the ET reaction, yet even in the presence of low values of $\Delta S^{\circ}$, the condition $\Delta G^{\ddagger} \cong \Delta H^{\ddagger}$ is expected to be valid, so that lower-boundary values of $\lambda_t$ can be determined on the basis of independent estimates of $\Delta G^{\circ}$ (*53*−*56*).

The standard midpoint potentials of the electron acceptor ($P_{700}^+$) and electron donor ($PC^I$) are 475 ± 10 mV (e.g., refs *33*, *53*, and *54*) and 360 ± 10 mV (*18*, *55*, *56*), respectively, so that the average value of $\Delta G^{\circ}$ is −115 meV. Following the studies of Drepper et al. (*33*) with isolated PS I, the free energy of $P_{700}^+$ reduction in the binary complex is reduced by ~45 meV, to account for differences in the binding constant for oxidized and reduced PC, so that the effective free energy $\Delta G^{\circ}_c = -70$ meV (where the subscript c will be used hereafter to refer to the $\Delta G^{\circ}$ of the ET reaction in the binary complex).

Assuming that (to a first approximation) the coupling with high-energy phonons is negligible in the temperature range investigated[2] and considering the values of $\Delta G^{\circ}$ (−115 meV) and $\Delta G^{\circ}_c$ (−70 meV), applying eq 6 leads to $\lambda_t$ estimates of 0.62 ± 0.01 and 0.55 ± 0.01 eV, respectively.[3] These values are in good agreement with the $\lambda_t$ of ≥545 meV determined by altering the driving force for the reaction (*30*), confirming the validity of the assumption that $\Delta G^{\ddagger} \cong \Delta H^{\ddagger}$. $\Delta G^{\ddagger}$ would lie in the range of 85−105 meV, using the value of $\lambda_t$ determined in ref *30* and the $\Delta G^{\circ}$ described above, indicating that the entropic contribution to the activation free energy is quite small.

The lower bounds of $\lambda_t$ can be considered accurate (within the high-temperature limit, which was also employed in ref *30*) if the measured lifetimes correspond to the actual reaction rate. In the most general case, the kinetics of reduction of $P_{700}^+$ in the binary complex are determined by the rates of both $P_{700}^+$ reduction ($k_1$)

[2]This approximation is substantially valid provided that mean phonon frequencies $\bar{v} \leq 150\ cm^{-1}$. Neglecting coupling with phonons might lead to underestimation of the value of $\lambda_t$.

[3]Deriving $\lambda_t$ from $\Delta G^{\ddagger}$ involves solving a second-order equation (eq 5), so two possible values of the reorganization energy are found. Independent of the choice of $\Delta G^{\circ}$, the low boundary value of $\lambda_t$ that numerically describes the activation barrier is ~10 meV. This would place $P_{700}^+$ reduction in the so-called inverted Marcus regime, a condition in which coupling with phonon modes cannot be neglected. However, 10 meV is too small to be considered reliable. Thus, we have excluded this value.

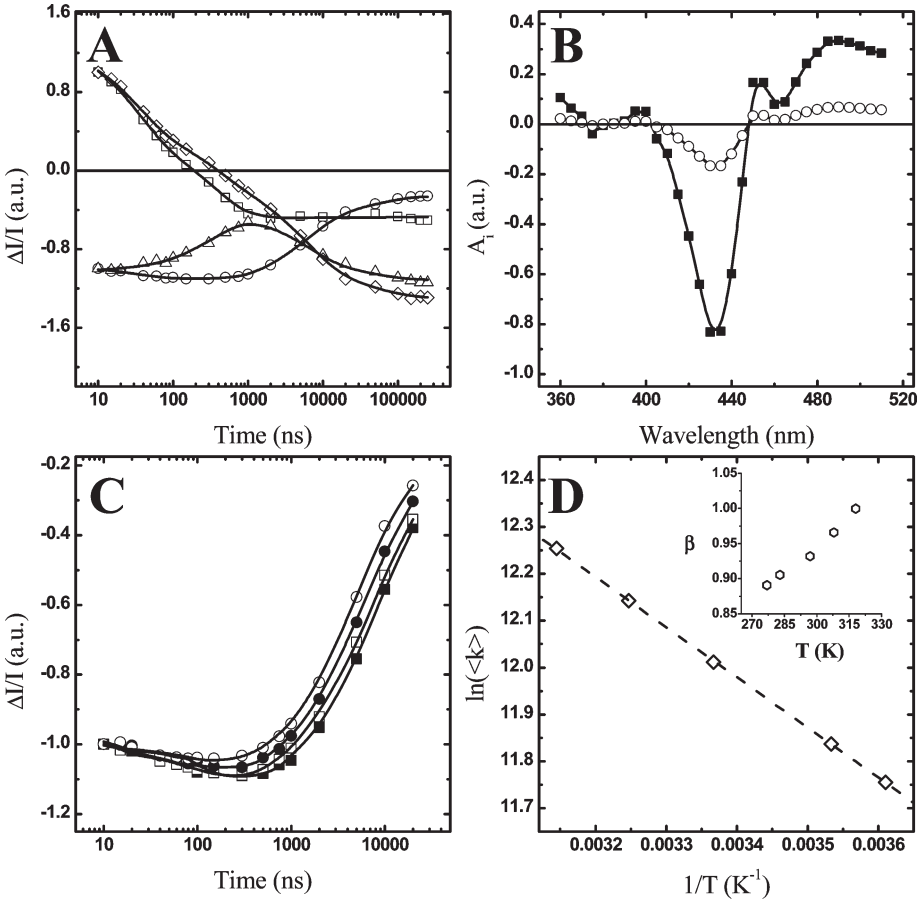


FIGURE 3: (A and B) Kinetics of flash-induced changes recorded on an extended time scale (5 ns to 300 $\mu$s) at 298 K. (A) Kinetics recorded at selected wavelengths at 298 K: 390 (□), 430 (○), 460 (△), and 480 nm (◇). Solid lines are the best fits. (B) DAS of the components with time constants of $6.3 \pm 0.1$ $\mu$s (■) and $55.6 \pm 0.4$ $\mu$s (○). The amplitudes are normalized to the sum of the two DAS. (C and D) Temperature dependence of $P_{700}^+$ reduction, fitted using the stretched exponential model function (in the 5 ns to 20 $\mu$s temporal interval): $f(t) = e^{-(t/\tau)\beta}$. (C) Kinetics monitored at 430 nm at 277 (■), 288 (□), 298 (●), or 305 K (○). Solid lines are best fits to the experimental results. (D) Arrhenius plot of average rate constant $\langle k \rangle$, which is obtained as $\langle k(T) \rangle^{-1} = [\tau(T)/\beta(T)]\Gamma[1/\beta(T)]$ (*49*), where $\Gamma$ is the gamma function. The slope was calculated as described in the legend of Figure 2 and yields a $\Delta H^{\ddagger}$ of 103 ± 1 meV. The inset in panel D shows the temperature dependence of stretching parameter $\beta$.

and the back-reaction (i.e., $P_{700}$ oxidation by $PC^{II}$, $k_2 = k_1 K_{eq}^{-1}(T)$). According to the simple reaction scheme $P_{700}^+ - PC^I \underset{k_2}{\overset{k_1}{\rightleftharpoons}} P_{700} - PC^{II}$ and neglecting the rate of dissociation of $PC^{II}$ from the complex, the $P_{700}^+$ reduction kinetics is expected to be monotonic and characterized by the observable lifetime $\tau_{obs}^{-1} = k_1 + k_2 = k_1[1 + K_{eq}^{-1}(T)]$. It is thus clear that $\tau_{obs}^{-1} \cong k_1$ when $K_{eq}(T)$ is large. This is definitely the case [i.e., $K_{eq}(T) > 60$] over the temperature range investigated if $\Delta G^\circ$ is calculated from the standard midpoint potentials of isolated complexes [i.e., assuming that the binding equilibrium of oxidized and reduced PC in vivo does not differ, as observed in vitro (*33*)]. However, even when the correction for the free energy of binding (i.e., using $\Delta G^\circ_c \sim -70$ meV) is taken into account, the value of $K_{eq}(T)$ lies in the range of 10−15, changing the rate by only ∼10%. Using this correction ($\Delta G^\circ_c = -70$ meV), $\Delta G^{\ddagger}$ is increased to 113 meV and $\lambda_t$ becomes 580 meV. The effect of the back-reaction upon the apparent lifetime would be more relevant if the free energy difference associated with the oxidation of $PC^I$ were to be decreased. However, in the case of previous studies in which the midpoint potential of $P_{700}^+/P_{700}$ was altered by site-directed mutagenesis (*30*), the driving force was increased with respect to the wild type.

Thus, in a manner independent of the details of the kinetic model employed to describe the data, and within the range of free energy values reported in the literature, the results obtained in this study confirm the previous conclusions based on altering the standard midpoint potential of $P_{700}^+/P_{700}$ (*30*). This shows that the rate of ET occurring between two bound redox proteins can be described in a manner analogous to those of intraprotein ET reactions. This strongly indicates the formation of a tight complex between PS I and $PC^I$, which is stable within the lifetime of the ET reaction (i.e., tens of microseconds).

The value calculated for $\lambda_t$ (≥0.54−0.6 eV) lies on the lower edge of the distribution for intracomplex ET reactions, which typically range from 0.7 to 1.3 eV (e.g., refs (*3*−*5*)). Such a low value is somewhat surprising, given that the redox center in PC is a copper ion, for which one would expect a larger value of $\lambda_t$ associated with reduction and oxidation, compared to those of large conjugated systems like hemes and chlorins (*1*−*5*). However, these high values of $\lambda_t$ are principally due to the large contribution of the rearrangement of water molecules within the metal's hydration sphere (which increases the reorganization energy of the reactant, $\lambda_i$) and the large dielectric constant of water (which increases the reorganization energy of the medium, $\lambda_o$). In cytochromes, the effect of solvent reorganization of the redox-active Fe atom is mitigated by coupling with the extended $\pi$-system of the porphyrin ring. The coordination sphere of Cu in PC includes donor bonds from the sulfur atoms in the thioether and thiolate groups of Met92 and Cys84, and from nitrogen atoms in the imidazole groups of His37 and His87 (e.g., ref *57*, for

the structure of *C. reinhardtii* PC). Thus, the electron spin density of the copper ion can, in part, be shared with the ligands in the coordinating sphere; in particular, the imidazole group has some aromatic character, so that it could contribute, in a manner analogous to that of the extended tetrapyrrole rings of Chls and hemes, to a lower $\lambda_t$ in the copper center of PC. In fact, mutations of the His ligands to the Cu center of PC are known to cause a remarkable slowing of the $P_{700}^+$ oxidation kinetics (e.g., refs *58* and *59*).

Moreover, the donor side of PS I immediately above $P_{700}$ is also very flat and hydrophobic, very much like the face of PC that binds there. It has been discussed before that this should lead to the exclusion of water molecules upon binding of PC to PS I (e.g., refs *25* and *60*), minimizing their impact on the reorganization energy within the PS I−$PC^I$ binary complex. The aromatic side chain of highly conserved Trp residues of PsaA (Trp651) and the PsaB (Trp627) also play a crucial role in modulating the affinity of the PC (and cyt $c_6$) binding to PS I (e.g., refs *25* and *60*). Both residues are close to the primary donor, so that the large hydrophobic patch at the interface between PC and PS I might serve not only in the optimization of binding but also in providing a preferential route for ET, while excluding water at the interface of the binary complex. In fact, site-directed mutations targeting PsaB Trp627 and PsaA Trp651 had the effect of both reducing the affinity of binding for PC (and cyt $c_6$) and slowing the fast phase of $P_{700}^+$ reduction by the residual fraction of bound donor (*25*, *60*).

*Is the Optimization of $P_{700}^+$ Reduction Physiologically Significant?* Ramesh and co-workers (*30*) calculated a maximal rate of $2.6 \times 10^6$ $s^{-1}$ for reduction of $P_{700}^+$ in vivo at 298 K, using the relationship $\Delta G° = -\lambda_t = -545$ meV. We obtained a similar, albeit slightly larger, value of $\sim 9 \times 10^6$ $s^{-1}$ from our independent estimation of $\lambda_t$ (0.55−0.62 eV), which yields the electronic coupling element ($|V_{AD}|$) value of ≈0.16 $cm^{-1}$. These values, while realistic, are at least somewhat inaccurate, because of the limited intervals of $\Delta G°$ and $T$ spanned in the two investigations. Nonetheless, these values can be used to calculate, to a first approximation, the rate constant of $P_{700}^+$ reduction for $\lambda_t$ of ≃1 eV, the average value for interprotein electron transfer, all other conditions remaining unchanged (including coupling with phonons).

Depending on the precise value of $|V_{AD}|$ used, the calculated maximal rate constant for ET would lie in the range of $1.5-3.5 \times 10^3$ $s^{-1}$. This value is ∼2 orders of magnitude smaller than the experimentally observed rate ($\sim 2 \times 10^5$ $s^{-1}$), indicating that the low value of $\lambda_t$ plays a significant role in the optimization of this electron transfer reaction, by lowering the activation barrier. In the more general case (i.e., when dropping the high-temperature limit), lowering of the barrier can also be the result of coupling ET with phonons of midhigh frequencies ($\bar{\nu} \geq 350$ $cm^{-1}$) when $\lambda_t \geq 0.8$ eV. For instance, the calculated ET rates for a $\lambda_t$ of 1 eV would yield observed lifetimes of $P_{700}^+$ reduction in the range of 250−750 μs. Alternatively, similar lengthening of the reaction kinetics is predictable by considering a communal "large" value of $\lambda_t$ (∼1 eV) when the frequency of the mean phonon is decreased from that of a "hard" environmental mode (i.e., ≥350 $cm^{-1}$) to that of a "soft" mode (≤50 $cm^{-1}$). The calculated rates of $P_{700}^+$ reduction in the 250−750 μs interval re not only asignificantly slower than those of the diffusion-limited process (50−70 μs, in vivo) but also enter the same time scale of $P_{700}^+$ reduction by charge recombination from either $PhQ^-$ (10−100 μs; reviewed in refs *43* and *44*) or $F_X$ (∼1 ms (*43*, *44*)). It seems unlikely that charge recombination would impose a limitation on electron transport through the whole chain under typical growth conditions, as ET from PhQ to $F_X$ and then to $F_A$ and $F_B$ takes place on the submicrosecond time scale (e.g., refs (*42*−*44*) and Figure 1). However, it is conceivable that the overall turnover rate of PS I, which is principally determined by donation of electrons from PC, might impose a kinetic bottleneck if it became comparable to that of cyt $b_6f$ turnover.

To evaluate semiquantitatively the possible limitation imposed by a "slow" reduction of $P_{700}^+$ by $PC^I$, we have simulated the reduction kinetics of $P_{700}^+$ considering two different scenarios that occur in photosynthetic organisms. The first corresponds to the situation found in eukaryotes, such as *C. reinhardtii*, in which the binding equilibrium of PC is largely in favor of the PS I−$PC^I$ binary complex, making the ∼6 μs phase the predominant $P_{700}^+$ reduction component. On the basis of the results obtained in this study, we estimated an equilibrium binding constant ($K_{bin}^{eq}$) of ∼6. The second scenario is that found in certain cyanobacterial strains, in which the lifetime of $P_{700}^+$ reduction is largely determined by the rate of formation of the PS I−$PC^I$ binary complex. In this case, $P_{700}^+$ is reduced with an average lifetime of ∼100 μs (e.g., refs (*18*−*20*)). Fast components (6−10 μs) of $P_{700}^+$ reduction are also observed in cyanobacteria in vivo and generally account for 15−20% of the total amplitude (e.g., refs *20*, *26*, and *48*), yielding $K_{bin}^{eq}$ values of ≈0.2. We have considered a simplified kinetic scheme (Figure 4) in which only two reactions are considered: (1) formation of the PS I($P_{700}^+$)−$PC^I$ complex and (2) the subsequent ET reaction leading to reduction of $P_{700}^+$ and oxidation of $PC^I$. As the dissociation of the PS I($P_{700}$)−$PC^{II}$ binary complex is not taken into account, this represents an only first-order approximation. The simplified model describes relatively well the biphasic reduction of $P_{700}^+$ for the eukaryotic-like as well as the prokaryotic-like scenario, both in terms of lifetime and in terms of relative amplitudes (Figure 4). In the two cases considered, the mean lifetime $\bar{\tau}$[4] has values of 103 and 258 μs when the electron transfer rate is determined with a $\lambda_t$ of 0.65. With an increase in the reorganization energy to 1 eV, the value of $\bar{\tau}$ increases to 147 μs (eukaryote-like scenario) or 455 μs (prokaryote-like scenario). This is determined by two factors, the lengthening of the lifetime associated with the electron transfer component (from ∼6 to ∼50 μs) and a small redistribution of the phases' amplitudes in favor of the diffusion-controlled rate. Interestingly, the prokaryotic-like scenario shows a larger sensitivity to a change in $\lambda_t$, the slowing of $P_{700}^+$ reduction being more evident than in the case of the eukaryotic-like scenario. This stems from the fact that, in this case, the pure ET phase is barely present. It is clear from this relatively simple approach that a decrease in the pure ET rate would lead to overall $P_{700}^+$ reduction times that are comparable to that of cyt $f$ turnover, which, under conditions in which photosynthetic ET is coupled to ATP synthesis, display average lifetime values of ∼200−300 μs for cyt $f$ oxidation and ∼2 ms for cyt $f$ and cyt $b$ reduction at the $Q_o$ site (e.g., refs *19* and *61*).

Hence, for the situations described above, one would expect to accumulate a fraction of $P_{700}^+$ under moderate steady-state illumination conditions. This might lead to an overall lowering of the rate of photosynthetic electron transport, as well as its

[4]The mean lifetime is defined as the first moment of the (normalized) function $f(t)$ describing the time dependence of the concentration of a given species. $\bar{\tau} = \int t f(t)\, dt$. The nondecaying component (Figure 4) has been omitted from the evaluation of $\bar{\tau}$.

A

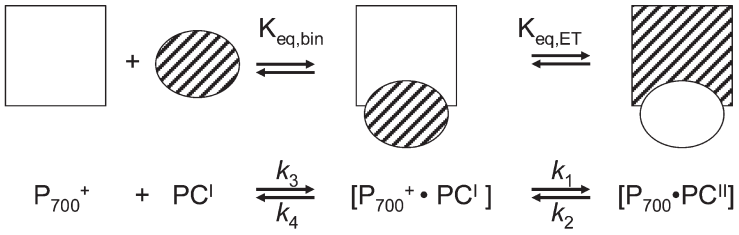


B

| | $k_1$ ($k_2$) $(\mu s)^{-1}$ | $k_3$ ($k_4$) $(\mu s)^{-1}$ | $\tau_1$, ($A_1$) ($\mu s$) | $\tau_2$ ($A_2$) ($\mu s$) | $\tau_3$ ($A_1$) ($\mu s$) |
|---|---|---|---|---|---|
| $\lambda_t = 0.6$ | 5.8 (159) | 65 (368) | 5.5 (0.80) | 65 (0.18) | - (0.02) |
| $\lambda_t = 1$ | 98 (2670) | 65 (368) | 48 (0.08) | 133 (0.90) | - (0.02) |
| | | | | | |
| $\lambda_t = 0.6$ | 5.8 (159) | 135 (158) | 5.8 (0.10) | 128 (0.72) | - (0.18) |
| $\lambda_t = 1$ | 98 (2670) | 135 (158) | 36 (-0.05) | 308 (0.87) | - (0.18) |

C

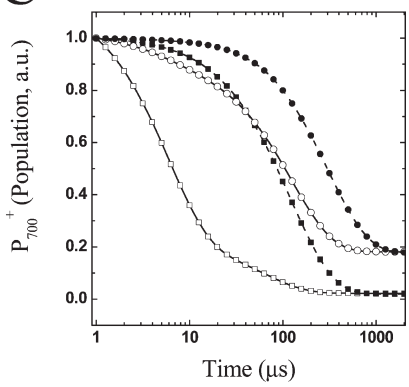


FIGURE 4: Simulations of the $P_{700}^+$ reduction by prebound and diffusible $PC^I$. (A) Schematic representation of the kinetic model employed in the calculations, the principal parameters of which are given in panel B for four considered scenarios. Note that $k_3$ is a second-order rate constant, while the other three are first-order constants. The system is solved for an approximate value of $k_3' = k_3\gamma_{PC^I}$, where $\gamma_{PC^I}$ is the molar fraction of unbound $PC^I$, which is thought not to change significantly during the course of the kinetics (i.e., $[PC^I] \gg [PS\ I]$). (C) Temporal evolution of the total $P_{700}^+$ molar fraction, calculated for four different scenarios: (□) $\lambda_t = 0.65$ meV, $\Delta G° = -85$ meV (this value of $\Delta G°$ is used in all of the simulations), and $K_{bin}^{eq} = 5.6$; (■) $\lambda_t = 1$ eV ($K_{bin}^{eq} = 5.6$); (○) $\lambda_t = 0.65$ meV and $K_{bin}^{eq} = 0.25$, and (●) $\lambda_t = 1$ eV ($K_{bin}^{eq} = 0.25$). Further details are given in the text.

efficiency, by the accumulation of photochemically incompetent PSI units. In this respect, the results of these simulations, although admittedly using a somewhat overly simplified reaction scheme, are qualitatively in agreement with the results obtained in mutants of *C. reinhardtii* either deficient or carrying substitutions in conserved residues of the N-terminal extension of the PsaF subunit, which is found only in eukaryotes and has been shown to be necessary for tight docking of PC and cyt $c_6$. These mutants display slow kinetics of $P_{700}^+$ reduction, and they are sensitive to light intensities exceeding 400 $\mu$E $m^{-2}$ $s^{-1}$ under aerobic conditions (*25*, *60*).

## SUPPORTING INFORMATION AVAILABLE

Decay-associated spectra from the fit of room-temperature kinetics, temperature dependence of the pre-exponential factors derived from the global-target fit of the experimental results, and temperature dependence of the lifetimes of nanosecond lifetimes derived from the global analysis of the experimental data. This material is available free of charge via the Internet at http://pubs.acs.org.

## REFERENCES


1. DeVault, D. (1980) Quantum mechanical tunnelling in biological systems. *Q. Rev. Biophys. 13*, 387–564.
2. DeVault, D. (1984) Quantum-Mechanical Tunnelling in Biological Systems , Cambridge University Press, Cambridge, U.K.
3. Marcus, R. A., and Sutin, N. (1985) Electron transfer in chemistry and biology. *Biochim. Biophys. Acta 811*, 265–322.
4. McLendon, G., and Hake, R (1992) Interprotein electron transfer. *Chem. Rev. 92*, 481–490.
5. Page, C. C., Moser, C. C., and Dutton, P. L. (2003) Mechanism for electron transfer within and between proteins. *Curr. Opin. Chem. Biol. 7*, 551–556.
6. Marcus, R. A. (1965) On the theory of oxidation-reduction reactions. IV. Unified treatment of homogeneous and electrode reactions. *J. Chem. Phys. 43*, 679–701.
7. Levich, V. G., and Dogonadze, R. R. (1959) Teiriya bezizluchatelnikh electronnikh perehodov mezhdu ionami v rastvorakh. *Dokl. Akad. Nauk SSSR 124*, 123–126.
8. Hopfield, J. J. (1974) Electron transfer between biological molecules by thermally activated tunneling. *Proc. Natl. Acad. Sci. U.S.A. 71*, 3640–3644.
9. Jortner, J. (1976) Temperature dependent activation energy for electron transfer between biological molecules. *J. Chem. Phys. 64*, 4860–4867.
10. Kuki, A., and Wolynes, P. G. (1987) Electron tunneling paths in proteins. *Science 236*, 1647–1652.
11. Beratan, D. N., Betts, J. N., and Onuchic, J. N. (1991) Protein electron transfer rates set by the bridging secondary and tertiary structure. *Science 252*, 1285–1288.
12. Gray, H. B., and Winkler, J. R. (1996) Electron Transfer in Proteins. *Annu. Rev. Biochem. 65*, 537–561.
13. Moser, C. C., Keske, J. M., Warncke, K., Farid, R. S., and Dutton, P. L. (1992) Nature of biological electron transfer. *Nature 355*, 796–802.
14. Warshel, A., and Parson, W. W. (1991) Computer simulations of electron-transfer reactions in solution and in photosynthetic reaction centers. *Annu. Rev. Phys. Chem. 42*, 279–309.
15. Blumberger, J. (2008) Free energies for biological electron transfer from QM/MM calculations: Methods, application and critical assessment. *Phys. Chem. Chem. Phys. 10*, 5651–5667.
16. Deisenhofer, J., and Norris, J. R. (1993) The Photosynthetic Reaction Center , Vol. II, Academic Press, San Diego.
17. Jasaitis, A., Rappaport, F., Pilet, E., Liebl, U., and Vos, M. H. (2005) Activationless electron transfer through the hydrophobic core of cytochrome *c* oxidase. *Proc. Natl. Acad. Sci. U.S.A. 102*, 10882–10886.
18. Haehnel, W. (1984) Plastocyanin. *Annu. Rev. Plant Physiol. 35*, 659–693.
19. Hope, A. B. (2000) Electron transfer amongst cytochrome *f*, plastocyanin and Photosystem I: Kinetics and mechanism. *Biochim. Biophys. Acta 1456*, 5–26.
20. Hervás, M., Navarro, J. A., and De La Rosa, M. A. (2003) Electron transfer between membrane complexes and soluble proteins in photosynthesis. *Acc. Chem. Res. 36*, 798–805.

21. Venturoli, G., Drepper, F., Williams, J. C., Allen, J. P., Lin, X., and Mathis, P. (1998) Effects of temperature and $\Delta G°$ on electron transfer from cytochrome $c_2$ to the photosynthetic reaction center of the purple bacterium *Rhodobacter sphaeroides*. *Biophys. J. 74*, 3226–3240.
22. Abresch, E. C., Paddock, M. L., Villalobos, M., Chang, C., and Okamura, M. Y. (2008) Interaction between cytochrome $c_2$ and the photosynthetic reaction center from *Rhodobacter sphaeroides*: Role of interprotein hydrogen bonds in binding and electron transfer. *Biochemistry 47*, 13318–13325.
23. Tiede, D. M., and Dutton, P. D. (1993) Electron transfer between bacterial reaction center and mobile *c*-type cytochromes. In The Photosynthetic Reaction Centre (Deisenhofer, J., and Norris, J. R., Eds.) pp 257−288, Academic Press, New York.
24. Setif, P. (2001) Ferredoxin and flavodoxin reduction by Photosystem I. *Biochim. Biophys. Acta 1507*, 161–179.
25. Sommer, F., Drepper, F., Haehnel, W., and Hippler, M. (2004) The hydrophobic recognition site formed by residues PsaA-Trp651 and PsaB-Trp627 of photosystem I in *Chlamydomonas reinhardtii* confers distinct selectivity for binding of plastocyanin and cytochrome $c_6$. *J. Biol. Chem. 279*, 20009–20017.
26. Durán, R. V., Hervás, M., De la Cerda, B., De la Rosa, M. A., and Navarro, J. A. (2006) A laser flash-induced kinetic analysis of in vivo photosystem I reduction by site-directed mutants of plastocyanin and cytochrome $c_6$ in *Synechocystis* sp. PCC 6803. *Biochemistry 45*, 1054–1060.
27. Fromme, P., Melkozernov, A., Jordan, P., and Krauss, N. (2003) Structure and function of photosystem I: Interaction with its soluble electron carriers and external antenna systems. *FEBS Lett. 555*, 40–44.
28. Adir, N., Axelrod, H. L., Beroza, P., Isaacson, R. A., Rongey, S. H., Okamura, M. Y., and Feher, G. (1996) Co-crystallization and characterization of the photosynthetic reaction center-cytochrome $c_2$ complex from *Rhodobacter sphaeroides*. *Biochemistry 35*, 2535–2547.
29. Axelrod, H. L., and Okamura, M. Y. (2005) The structure and function of the cytochrome $c_2$: Reaction center electron transfer complex from *Rhodobacter sphaeroides*. *Photosynth. Res. 85*, 101–114.
30. Ramesh, V. M., Guergova-Kuras, M., Joliot, P., and Webber, A. N. (2002) Electron transfer from plastocyanin to photosystem I reaction center mutants with increased potential of the primary donor in *Chlamydomonas reinhardtii*. *Biochemistry 41*, 14652–14658.
31. Lin, X., Williams, J. C., Allen, J. P., and Mathis, P. (1994) Relationship between rate and free energy difference for electron transfer from cytochrome $c_2$ to the reaction center in *Rhodobacter sphaeroides*. *Biochemistry 33*, 13517–13523.
32. Venturoli, G., Mallardi, A., and Mathis, P. (1993) Electron transfer from cytochrome $c_2$ to the primary donor of *Rhodobacter sphaeroides* reaction center. A temperature dependence study. *Biochemistry 32*, 13245–13253.
33. Drepper, F., Hippler, M., Nitscke, W., and Haenel, W. (1996) Binding Dynamics and Electron Tranfer between Plastocyanin and Photosystem I. *Biochemistry 35*, 1282–1295.
34. Beal, D., Rappaport, F., and Joliot, P. (1999) A new high-sensitivity 10-ns time-resolution spectrophotometric technique adapted to in vivo analysis of the photosynthetic apparatus. *Rev. Sci. Instrum. 70*, 202–207.
35. Beechem, J. M. (1992) Global analysis of biochemical and biophysical data. *Methods Enzymol. 210*, 37–54.
36. Joliot, P., and Joliot, A. (1999) *In vivo* analysis of the electron transfer within Photosystem I: Are the two phylloquinones involved? *Biochemistry 38*, 11130–11136.
37. Guergova-Kuras, M., Boudreaux, B., Joliot, A., Joliot, P., and Redding, K. (2001) Evidence for two active branches for electron transfer in Photosystem I. *Proc. Natl. Acad. Sci. U.S.A. 98*, 4437–4442.
38. Byrdin, M., Santabarbara, S., Gu, F., Fairclough, W. V., Heathcote, P., Redding, K., and Rappaport, F. (2006) Assignment of a kinetic component to electron transfer between iron-sulfur clusters $F_X$ and $F_{A/B}$ of Photosystem I. *Biochim. Biophys. Acta 1757*, 1529–1538.
39. Santabarbara, S., Jasaitis, A., Byrdin, M., Gu, F., Rappaport, F., and Redding, K. (2008) Additive effect of mutations affecting the rate of phylloquinone reoxidation and directionality of electron transfer within Photosystem I. *Photochem. Photobiol. 84*, 1381–1387.
40. Agalarov, R., and Brettel, K. (2003) Temperature dependence of biphasic forward electron transfer from the phylloquinone(s) PhQ in photosystem I: Only the slower phase is activated. *Biochim. Biophys. Acta 1604*, 7–12.
41. Schlodder, R., Falkenberg, K., Gergeleit, M., and Brettel, K. (1998) Temperature dependence of forward and reverse electron transfer from $PhQ^-$, the reduced secondary electron acceptor in Photosystem I. *Biochemistry 37*, 9466–94676.
42. Santabarbara, S., Heathcote, P., and Evans, M. C. W. (2005) Modelling of the electron transfer reactions in Photosystem I by electron tunnelling theory: The phylloquinones bound to the PsaA and the PsaB reaction centre subunits of PS1 are almost isoenergetic to the iron-sulfur cluster $F_X$. *Biochim. Biophys. Acta 1708*, 283–310.
43. Brettel, K. (1997) Electron transfer and arrangement of the redox cofactor in Photosystem I. *Biochim. Biophys. Acta 1318*, 322–373.
44. Brettel, K., and Leibl, W. (2001) Electron transfer in photosystem I. *Biochim. Biophys. Acta 1507*, 100–114.
45. Sigfridsson, K. (1998) Plastocyanin, an electron transfer protein. *Photosynth. Res. 57*, 1–28.
46. Sigfridsson, K., Hansson, O., Karlsson, B. G., Baltzer, L., Nordling, M., and Lundberg, L. G. (1995) Spectroscopic and kinetic characterization of the spinach plastocyanin mutant Typ83-His: A histidine residue with a high pK value. *Biochim. Biophys. Acta 1228*, 28–36.
47. Sigfridsson, K., He, S., Modi, S., Bendall, D. S., Gray, J., and Hansson, O. (1996) A comparative flash-photolysis study of electron transfer from pea and spinach plastocyanins to spinach Photosystem I. A reaction involving a rate-limiting conformational change. *Photosynth. Res. 50*, 11–21.
48. Díaz, A., Hervás, M., Navarro, J. A., Rosa, M. A., and Tollin, G. (1994) A thermodynamic study by laser-flash photolysis of plastocyanin and cytochrome $c_6$ oxidation by photosystem I from the green alga *Monoraphidium braunii*. *Eur. J. Biochem. 222*, 1001–1007.
49. Haenel, W., Doring, G., and Witt, H. T. (1971) Reaction between chlorophyll-$a_I$ and its primary electron donors in photosynthesis. *Z. Naturforsh., B 26*, 1171–1174.
50. Hiyama, T., and Ke, B. (1971) A new photosynthetic pigment, P430: Its possible role as the primary electron acceptor of Photosystem I. *Proc. Natl. Acad. Sci. U.S.A. 68*, 1010–1013.
51. Berbetan-Santos, M. N., Bodunov, E. N., and Valeur, B. (2005) Mathematical functions for the analysis of luminescence decays with underlying distributions 1. Kohlrausch decay function (stretched exponential). *Chem. Phys. Lett. 315*, 171–182.
52. Williams, G., and Watts, D. C. (1970) Non-Symmetrical Dielectric Relaxation Behavior Arising from a Simple Empirical Decay Function. *Trans. Faraday Soc. 66*, 80–85.
53. Evans, M. C. W., Sihra, C. K., and Slabas, A. R. (1977) The oxidation-reduction potential of the reaction-centre chlorophyll ($P_{700}$) in Photosystem I. Evidence for multiple components in electron-paramagnetic-resonance signal I at low temperature. *Biochem. J. 162*, 75–85.
54. Webber, A. N., and Lubitz, W. (2001) $P_{700}$: The primary electron donor of photosystem I. *Biochim. Biophys. Acta 1507*, 61–79.
55. Katoh, S., Shiratori, I., and Takamiya, A. (1962) Purification and some properties of spinach plastocyanin. *J. Biochem. 51*, 32–40.
56. Sanderson, D. G., Anderson, L. B., and Gross, E. L. (1986) Determination of the redox potential and diffusion coefficient of the protein plastocyanin using optically transparent filar electrodes. *Biochim. Biophys. Acta 852*, 269–278.
57. Redinbo, M. R., Cascio, D., Choukair, M. K., Rice, D., Merchant, S., and Yeates, T. O. (1993) The 1.5-Å crystal structure of plastocyanin from the green alga *Chlamydomonas reinhardtii*. *Biochemistry 32*, 10560–10567.
58. Nordling, M., Sigfridsson, K., Young, S., Lundberg, L. G., and Hansson, O. (1991) Flash-photolysis studies of the electron transfer from genetically modified spinach plastocyanin to Photosystem I. *FEBS Lett. 291*, 327–330.
59. Haehnel, W., Jansen, T., Gause, K., Klösgen, R. B., Stahl, B., Michl, D., Huvermann, B., Karas, M., and Herrmann, R. G. (1994) Electron transfer from plastocyanin to Photosystem I. *EMBO J. 13*, 1028–1038.
60. Sommer, F., Drepper, F., and Hippler, M. (2002) The luminal helix l of PsaB is essential for recognition of plastocyanin or cytochrome $c_6$ and fast electron transfer to Photosystem I in *Chlamydomonas reinhardtii*. *J. Biol. Chem. 277*, 6573–6581.
61. Berry, E. A., Guergova-Kuras, M., Huang, L. S., and Crofts, A. R. (2000) Structure and function of cytochrome *bc* complexes. *Annu. Rev. Biochem. 69*, 1005–10075.